Single-cell RNA sequencing of conditional *Pten* knockout neurons in mice

Marek Svoboda[1], **Bryan Luikart**[2], **and Giovanni Bosco**[2,✉]

[1]Quantitative Biomedical Sciences Program, Geisel School of Medicine, Dartmouth College
[2]Molecular and Systems Biology Program, Geisel School of Medicine, Dartmouth College

PTEN is a well-known tumor suppressor whose mutations are also strongly associated with Autism Spectrum Disorder (ASD). The activity and function of PTEN in neurons have been studied extensively in various settings, whereas animal models offer the best opportunity to experimentally modify and test the role of PTEN in neuronal development *in vivo*. On the molecular level, PTEN's importance in the mTOR pathway's suppression is well-known but many other interactions have been suggested and yet others likely remain undiscovered. Therefore, to systematically explore the regulatory landscape downstream of PTEN on the genetic level, we have set out to establish a single-cell RNA sequencing (scRNA-seq) workflow to measure gene expression changes as a result of knocking out the *Pten* gene *in vivo*. We were able to collect brain tissue from four conditionally knocked out mouse samples and dissociate them into single live cells, which were subsequently flow-sorted and a scRNA-seq library was prepared. All of these steps were completed in a single day, yielding sequencing data from hundreds of cells suitable for cell clustering, cell type identification, and differential expression measurements. Having demonstrated its feasibility, this approach promises to aid hypothesis generation and discovery in mapping the function of *Pten* as well other genes whose regulatory networks remain to be fully defined.

single-cell RNA sequencing | NGS | PTEN | Conditional Knockout | mouse
Correspondence: ***Giovanni.Bosco@Dartmouth.edu***

Introduction

Phosphatase and TENsin homolog (*PTEN*) was first identified as the gene responsible for Cowden syndrome located on chromosome 10q22-23 (1). Its function was soon established as a tumor suppressor missing in endometrial carcinoma (2), glioma (3), kidney (4), breast (5), and prostate cancers (6, 7). Dominant germline *PTEN* mutations have been also linked to other tumor syndromes: Bannayan-Riley-Ruvalcaba syndrome (8), Proteus syndrome (9), and Proteus-like syndrome (10). Subsequently, these phenotypically heterogeneous diseases were combined under the diagnostic umbrella of *PTEN* Hamartoma Tumor Syndrome (PHTS) (11, 12). Soon after its discovery, mutations in *PTEN* were also associated with autism spectrum disorder (ASD) (13). *PTEN* mutations are now identified in about 10% of people with ASD and macrocephaly (14, 15), making it one of the most commonly mutated genes in these patients, which account for about 20% of all ASD cases (16). Apart from other pathogenic signs like seizures, ataxia, and Lhermitte-Duclos disease (17), macrocephaly is one of the hallmark signs of individuals carrying germline *PTEN* mutations, with or without PHTS, underscoring the importance of this gene in neurons, where it has been found to be important for normal function, development, and morphology (18–20) and its loss leads to their precocious differentiation, mislocation, hypertrophy, hyperexcitability, and increased survival (21–26).

Several mouse models have been created to study PTEN function. While homozygous *Pten* loss leads to embryonic lethality, *Pten* heterozygous mice have high tumor incidence (27–29). Mouse models for studying Pten's role in neurons include its conditional knockout (cKO, $Pten^{flox/flox}$) (30), short hairpin RNA knockdown (24), and nuclear excluded PTEN ($Pten^{M3M4}$) (31). These mice reproduce the phenotypes seen in PTEN-ASD patients including macrocephaly, seizures, and abnormal social interactions (16, 23, 32).

Thanks to these mouse models, we can study PTEN function on the cellular and molecular level. PTEN has been described as a lipid and protein phosphatase (17, 33). Its most studied function is dephosphorylation of PIP_3, which results in regulation of the PI3K-Akt-mTORC1 pathway (34, 35) (Figure 1A). Accordingly, many of the *Pten* KO-associated changes are rescued or prevented when neurons are treated with rapamycin, an mTOR inhibitor (36). However, our previous work shows that excessive microtubular (MT) polymerization, which mediates abnormal neural process formation in *Pten* KO neurons, is not rescued by acute rapamycin treatment (Figure 1B, *unpublished*). This suggests that PTEN exerts its regulatory activity in neurons through other pathways.

While the effects of PTEN's *lipid* phosphatase activity on PIP_3 have been well studied, little is known about the significance of PTEN's *protein* phosphatase activity. PTEN protein phosphatase has been suggested to regulate cell migration through focal adhesion kinase (FAK) (37) and Shc (38) in glioblastoma (GBM), neural stem cell differentiation through cyclic AMP response element-binding (CREB) protein (26, 39) (Figure 1A), neuronal spine density (40) and tumor suppression of GBM (41) by autodephosphorylation, and cell metabolism through insulin receptor substrate-1 (IRS-1) (42).

Additionally, interactions with other genes seem to be of great importance for the penetrance of *PTEN*-associated pathology. For example, males are four times more likely than females to be diagnosed with ASD (44, 45) and similar pattern is found in *PTEN*-specific cases (13, 46, 47). In mice, behavioral deficits in both *Pten* haploinsufficient (32) and cytoplasm-predominant (48) models are sex-specific as well. Similarly, penetrance of *Pten* haploinsufficiency-associated tumors depends on genetic background (49). Nuclear localization of PTEN (50) and its interactions with mul-

tiple targets (37, 39) indicate it may have indirect effects on transcriptional regulation. Taken together, these studies strongly suggest important interactions between *PTEN* and other genes crucial for ASD and other pathologies, whose molecular mechanisms are yet to be elucidated.

Despite the abundant evidence that PTEN interacts with other proteins and genes, our knowledge of PTEN's causal involvement in neural disease phenotypes is lacking. Only a systematic investigation of PTEN's regulatory effects accounting for their diversity and temporal dynamics can ensure that we obtain a complete picture of its downstream mediators and hence potential pharmacological targets. Therefore, we developed a single-cell RNA sequencing (scRNA-seq) protocol to measure gene expression in a conditional knockout (cKO) *Pten* mouse model of autism to study transcriptional states during neuronal development *in vivo* (51). This approach will allow us to analyze the resulting data using a variety of computational methods, such as differential expression (DE), cell clustering, cell type assignment, and pseudotemporal ordering (Figure 1C), to identify the cell states present in *PTEN*-associated ASD and the regulatory pathways downstream of PTEN through which they arise. To our knowledge, scRNA-seq has not been previously used to study transcriptomic changes in selectively *Pten*-disrupted cells.

Results

Infection and collection of *Pten* conditional knockout mouse neurons developed *in vivo*

We used homozygous *Pten* conditional knockout (cKO) mice, in which *Pten* gene exons 4 and 5 were flanked by loxP sequences ($Pten^{flox/flox}$, Figure 1D) (30). This portion of *Pten*, encoding the core phosphatase motif, is excised in

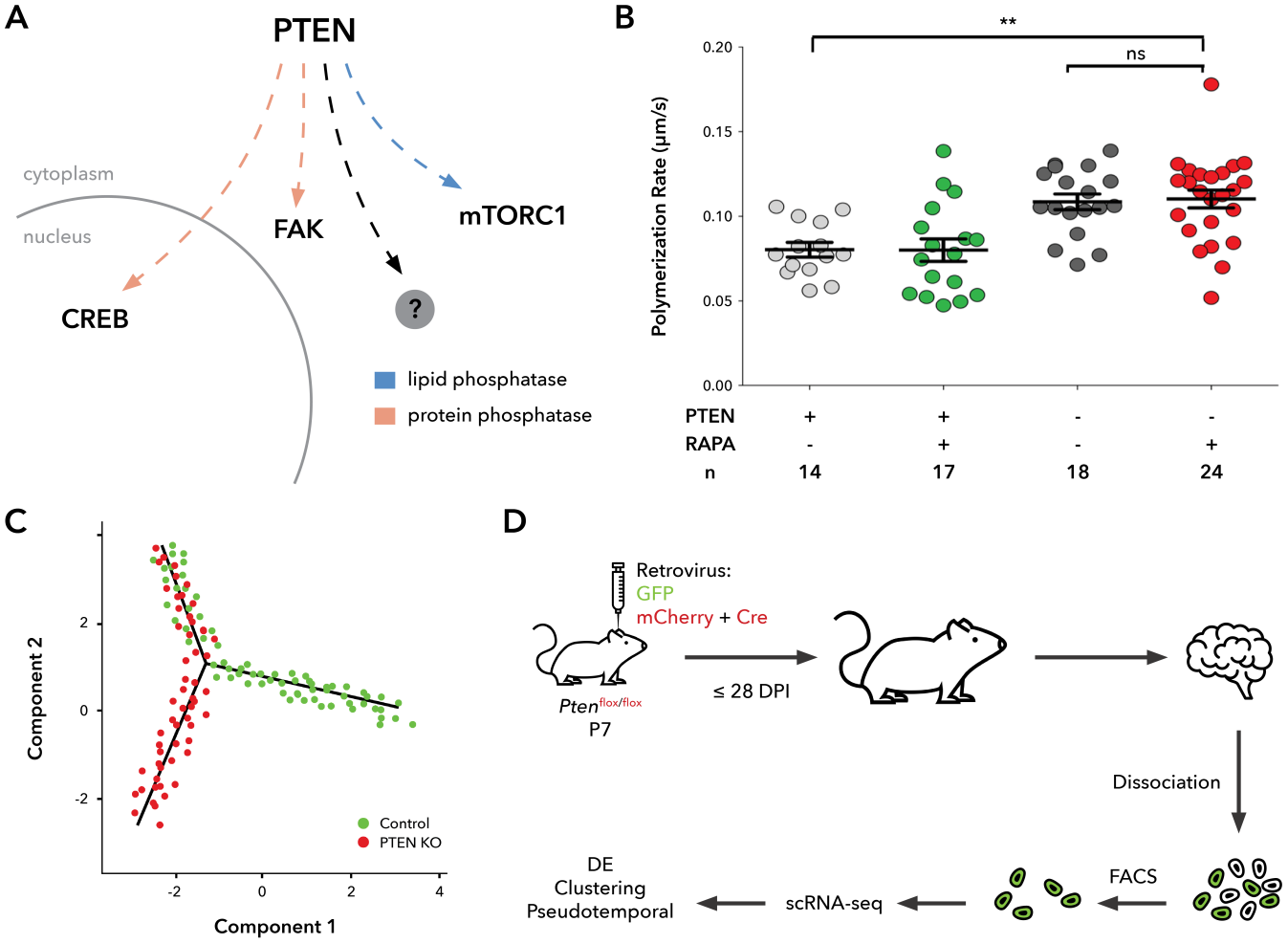

Figure 1. Identification of novel *Pten*-dependent pathways using scRNA-seq.
A. Neuronal pathways regulated by PTEN lipid and protein phosphatase activity. While the effects of PTEN's lipid phosphatase activity on the mTORC1 pathway have been well studied, little is known about the significance of PTEN's protein phosphatase activity. It has been suggested to regulate cell migration through focal adhesion kinase (FAK)8 and neural stem cell differentiation through cyclic AMP response element-binding (CREB) protein (39).
B. Acute rapamycin treatment ("RAPA +") does not correct the microtubular polymerization rate in *Pten* KO ("PTEN -") neurons. (Unpublished data provided by Stephanie Getz.)
C. The expected outcome of pseudotemporal ordering of individual cells using the Monocle 2 (43) algorithm. *Pten* KO neurons are expected to deviate from Control neurons' developmental trajectory of ordered cell states.
D. Flowchart outlining the experimental design: mice are injected with retroviral particles containing either pRubiG (GFP) or pRubiC-T2A-Cre (mCherry and Cre separated by a self-cleaving peptide, T2A) around post-natal day 7 (P7). Cells are collected 28 days post-injection (28 DPI), dissociated, and enriched for GFP+ (control) or mCherry+ (KO) cells before scRNA-seq and subsequent computational analysis.

the presence of Cre, resulting in *Pten* KO. We targeted hippocampal dentate gyrus (DG), which is one of the structures impaired in ASD (52) and whose continued neurogenesis into adulthood (in both mice and humans) facilitates study of neuronal development and makes it a potential candidate for future treatment targeting. DG in these mice was therefore injected on post-natal day 7 with retroviral particles, which selectively target dividing cells. These particles carried either Cre and mCherry (KO) or only GFP (control). This strategy allows for precise control over the cell population and timing of the KO. Brain tissue was subsequently collected 28 days post injection, eclipsing the peak neurogenesis in mouse hippocampus (53) and allowing any morphological changes to take place after *Pten* KO (25).

The collected brain tissue was subsequently separated into single cells through gentle dissociation. We optimized the timing of this process through several iterations to be able to process up to four samples in a single day to minimize any batch effects and at the same time, to maximize the number of surviving cells for each sample. The following samples were collected: a GFP+ male control (M_GFP), a Cre-mCherry+ male KO (M_mCherry-Cre), a GFP+ female control (F_GFP), and a Cre-mCherry+ female KO (F_mCherry-Cre). All samples had to be staggered while being processed during each precisely timed individual step to ensure that all the steps starting with tissue collection of *in vivo* neurons up to single-cell RNA library preparation could be carried out in a single day. Keeping the timing at a minimum aimed to limit the effect of handling on the final measurement of gene expression in the live neurons.

Cell sorting through flow cytometry

The dissociated cells were then subjected to fluorescence-activated cell sorting (FACS) using the appropriate lasers and gating parameters to select only those single cells (i.e. singlets) that survived the extraction and dissociation process described above (i.e. low DAPI) and had been fluorescently labeled *in vivo* (GFP or mCherry positive for the control or KO cells, respectively).

Aiming to extract as many live neurons as possible, we were able to dissociate about $1,000,000$ cells from each of the four samples studied. Cells in each sample were then sorted based on four sequential gates in the following combinations of parameters, which were consistent across all samples: FSC (forward scatter) -A (area) vs. SSC (side scatter) -A, which yielded between $11-15.6\%$ of all cells; FSC-H (height) vs. FSC-W (width), which yielded $96.7-99.6\%$ of the remaining cells; SSC-H vs. SSC-W, which yielded $95.6-98.5\%$ of the remaining cells; and GFP (green fluorescent protein) -A vs. DAPI-A, through which only $0.8-1.7\%$ of the remaining cells were selected (Table 1 and Figure 2). This resulted in only $0.1-0.3\%$ of the total number of cells having been positively selected by FACS, yielding approximately between $1,000-3,000$ of the original about $1,000,000$ total cells sorted per sample.

Population	#Cells	%Parent	%Total
All Events	$10,000$	NA	100.0
P1 (FSC-A vs. SSC-A)	$1,559$	15.6	15.6
P2 (FSC-H vs. FSC-W)	$1,541$	98.8	15.4
P3 (SSC-H vs. SSC-W)	$1,513$	98.2	15.1
P4 (GFP-A vs. DAPI-A)	26	1.7	0.3

Table 1. Proportions of cells filtered by FACS in sample 2F_GFP.
Table showing the numbers and relative (%Parent) and absolute (%Total) proportions of cells selected by each subsequent FACS gate in a sub-sample of $10,000$ cells, as shown in Figure 2.

Single cell RNA sequencing quality control filtering

The flow-sorted cells were then used for single-cell RNA library preparation using the standard 10X Genomics Chromium protocol followed by next-generation sequencing. Sequencing reads were subsequently decomplexed and aligned to the mouse genome, yielding a gene-cell matrix for each sample. The final number of cells detected by single-cell RNA sequencing (scRNA-seq) per sample ranged between $314-640$, the mean number of sequencing reads per cell was between $143,802-329,980$, and the median number of genes detected per cell was between $27-2,198$ (Table 2). Based on the significantly lower median numbers of genes detected per cell, the samples from the female mice were determined to be of insufficient quality and were not included in the subsequent analyses.

As is customary in scRNA-seq data analysis (54), the cells were further filtered based on the metrics discussed above, as well as the content of mitochondrial genes detected (Figure 3A). Because too few genes per cell are usually associated with low cell quality or background measurement and too many genes per cell suggest the presence of doublets, we removed cells that contained less than 200 or more than 5,000 genes (Figure 3B). Similarly, cells with an excessively high proportion of mitochondrial genes suggest loss of mitochondrial integrity associated with cell death and therefore contamination secondary to cell membrane disruption. Hence, cells that contained more than 20% mitochondrial genes were also removed. After this quality control (QC) filtering step, 193 control and 240 KO cells from the male samples were left in the dataset.

Cell clustering and gene expression patterns detected

Clustering analysis of the *Pten* KO (n = 240) and control (n = 193) neurons from the male mice showed significant overlap between *Pten* KO and control cell populations, suggesting that transcriptome of some cells did not change signifi-

Sex	Condition	Cells	Reads/c	Genes/c
M	GFP (Control)	314	$307,449$	$1,378$
M	mCherry-Cre (KO)	322	$329,980$	$2,198$
F	GFP (Control)	640	$143,802$	27
F	mCherry-Cre (KO)	377	$299,249$	95

Table 2. Summary statistics for the scRNA-seq samples before filtering.
The columns denote the mouse sex, sample condition, total number of cells, the mean number of reads per cell, and the median number of genes per cell detected in each respective scRNA-seq library.

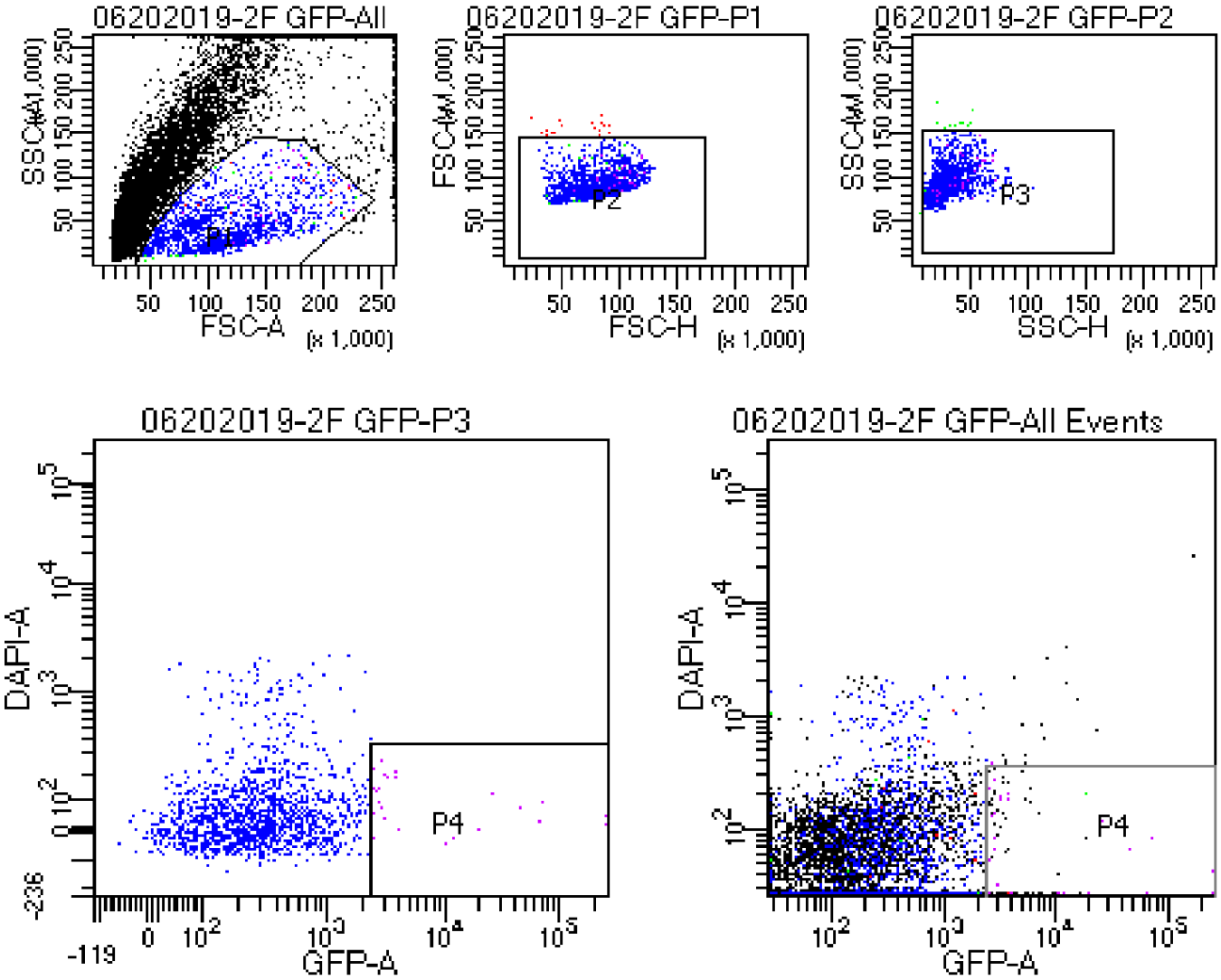

Figure 2. Fluorescence-activated cell sorting (FACS) of cKO neurons from sample 2F_GFP, using four separate gates.
The four gates used for cell sorting. Top: P1 - FSC (forward scatter) -A (area) vs. SSC (side scatter) -A, singlets inside gate; P2 - FSC-H (height) vs. FSC-W (width), singlets inside gate; P3 - SSC-H vs. SSC-W, singlets inside gate. Bottom: P4 - GFP (green fluorescent protein) -A vs. DAPI (4',6-diamidino-2-phenylindole) -A, GFP positive alive cells inside gate; left: only cells selected by all previous gates are shown, right: all cells are shown.

cantly after *Pten* KO (Figure 3A). Notably, however, each of the two experimental groups also exhibited a transcriptionally unique cell population not found in the other group, suggesting a detectable effect associated with knocking out of *Pten* in a subset of cells. Namely, the control sample contained a cluster of neuroepithelial cells not found in the KO sample and, similarly, the KO sample contained one cluster of neuroepithelial cells and one cluster of neurons not found in the control sample (Figure 3B). Knockout of *Pten* during neuronal development may therefore lead to a change in the cell differentiation process, whereby the transcriptional state of some neuroepithelial cells (i.e., the neural stem cells) is altered and may also lead to the development of neurons with an abnormal transcriptional profile.

Gm47283 and *Plp1* were the top two most significantly differentially expressed genes between the control and KO samples in both neurons and neuroepithelial cells, followed by *Osm* and *Itm2a* in these cell types, respectively (Figure 3C). The *Plp1* gene, which is X-linked and encodes for the proteolipid protein integral to myelin formation (55), was most highly expressed in the neuronal cluster specific to the control sample (Figure 3D). Conversely, the *Itm2a* gene, which encodes for Integral membrane protein 2A shown to be important in chondro-osteogenic and myogenic differentiation (56), was most highly expressed in the two clusters specific to the KO sample. It is also notable that the gene that was one of the most differentially expressed genes in neurons but not in neuroepithelial cells, *Osm*, encodes the Oncostatin M protein, which has been found to suppress the growth of several oncogenic cell lines (57), activity comparable to that of the tumor suppressor PTEN. The *Pten* gene was not detected as differentially expressed between the control and KO samples in any of the cell types detected, nor among all the cells overall.

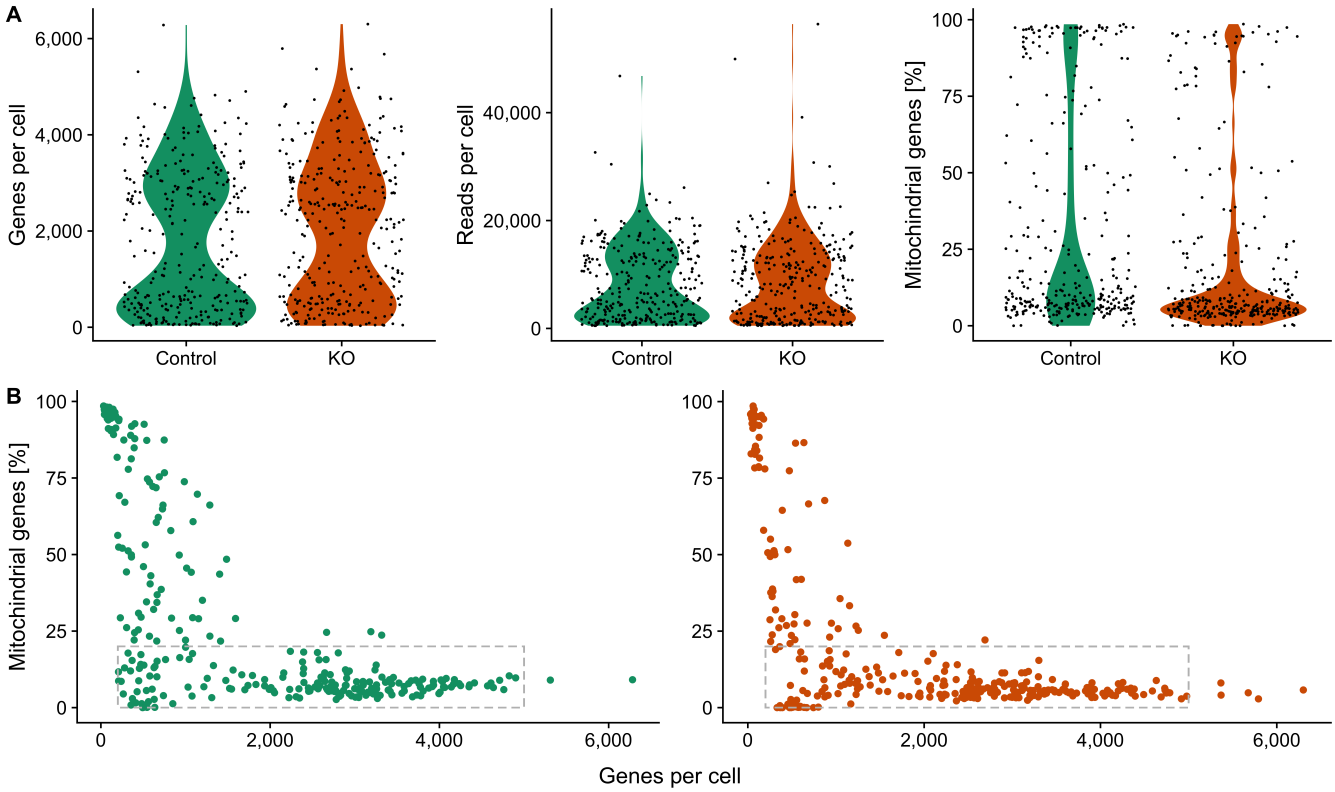

Figure 3. Quality control (QC) measurements of the male samples.
A. Violin plots of the number of genes, total number of RNA reads, and percentage of mitochondrial genes per cell in each sample. Samples depicted: 1M_GFP (control - green) and 5M_mCherry (KO - orange).
B. Plots of the number of genes vs. percentage of mitochondrial genes per cell in each of the samples. Cells enclosed in the gray boxes are those that passed the QC filtering - i.e., containing between $200 - 5,000$ genes and less than 20% of mitochondrial genes detected. The colors are the same as in **A.** - left: control; right: KO.

Discussion

As the role of PTEN in neurons remains to be elucidated on the molecular level, in this study, we have developed an unbiased approach to explore the regulatory pathways downstream of PTEN *in vivo* and demonstrated the feasibility to collect up to four samples in a single day using this protocol. Specifically, we explored the KO-induced cellular changes using scRNA-seq to capture the alterations in transcriptional states during neuronal development. To our knowledge, *Pten* mutations in neurons have not been previously studied using scRNA-seq.

We have identified an absence of a specific subset of neuroepithelial cells and the emergence of a different group of neuroepithelial cells as well as neurons as a result of knocking out *Pten*. We have also detected genes that were differentially expressed between the samples, some of which were specific to neurons. This data underscores the importance of the scRNA-seq approach, as these differences were only found in a subset of cells and would likely be blunted or completely lost using bulk RNA-seq technology.

Additional scRNA-seq experiments will be necessary to optimize this technique and obtain data from enough cells that pass the downstream quality control (QC) checks for further analyses. One of the potential issues of this study is that *Pten* was not differentially expressed between the samples, as would be expected from its targeted knockout. While the introduction of Cre has been previously shown to significantly decrease the amount of PTEN protein in the cells from the mouse model used (25), it is conceivable that the amount of *Pten* mRNA transcripts is not significantly altered by the excision of the gene's exons 4 and 5, which would explain the lack of its differential expression on the transcriptomic level. It is possible, however, that instead, the cells analyzed by scRNA-seq in the KO sample did not exhibit the intended suppression of PTEN expression, which might have occurred in several ways.

One of the most significant problems encountered during the tissue preparation for scRNA-seq was the noted faintness of the expressed fluorophores (GFP and mCherry). It is known that the endogenously expressed fluorophores, secondary to the *in vivo* retroviral infection of neurons, are relatively lowly luminescent and are therefore often amplified by immunohistochemistry in the *in vitro* microscopy experiments in our laboratory. During FACS sorting, a bimodal distribution of luminescence would be expected, clearly distinguishing the distinctly luminescent cells from those that do not contain the fluorophore, which was not observed during our experiment's FACS sorting (Figure 2, gate P4).

Additionally, we were unable to detect Cre in the KO sample as an internal control of a successful viral construct infection and expression. This was most likely because the viral construct used lacks a poly(A) signal, the addition of which would enable the detection of Cre in the sequencing data from future experiments.

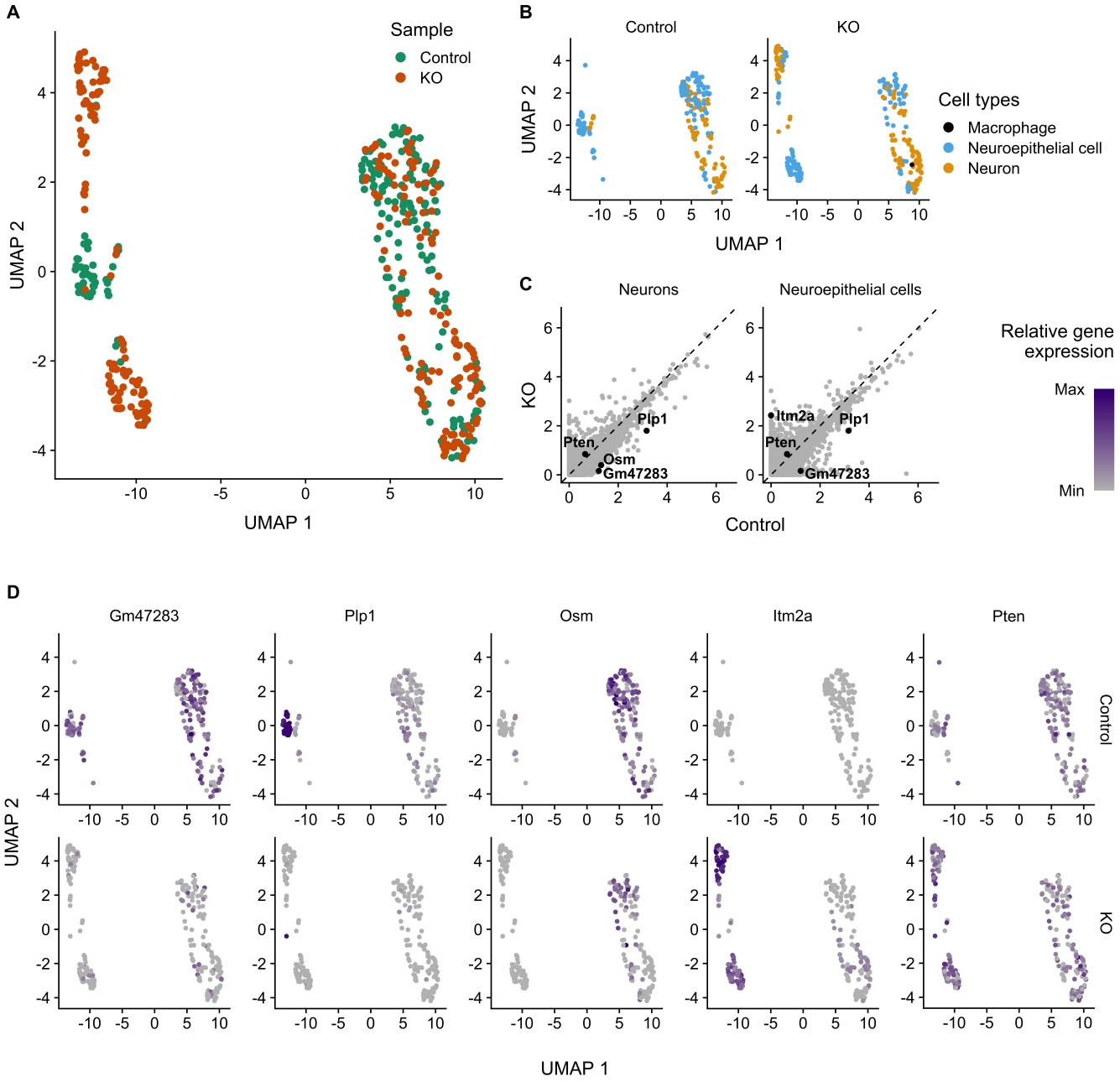

Figure 4. Clustering analysis of the male samples.
A. UMAP plot of all the cells that passed the QC, colored by the sample or origin.
B. UMAP plots of cells split by sample and colored by the cell types detected: neurons, neuroepithelial cells, and a macrophage. (Only one cell in the KO sample and none in the control sample was classified as a macrophage.)
C. Plots of normalized gene expressions in the control vs. KO sample, in the two major cell types detected. *Pten* and the top three genes most significantly differentially expressed between the samples in neurons and neuroepithelial cells are highlighted. The gray dashed line represents equal expression between the samples.
D. UMAP plots colored by the relative expression of the genes highlighted in **C.**, split by the sample of origin. The differential expressions between the control vs. KO sample of all these genes were statistically significant, except for *Pten*.

We also suspect that the low cell yields between cell dissociation and scRNA-seq preparation were caused by excessive cell death. Cell dissociation of live neurons, which possess numerous processes, is notoriously more problematic than that of regularly shaped cells or those that are less tightly interconnected with their milieu. It is therefore common to extract neuronal nuclei instead, which has several advantages (58). Neuronal dissociation is rendered faster, as it does not require excessive care to maintain the cell membrane integrity to keep cells alive and the nuclear membrane itself is more sturdy. Additionally, nuclei can be readily dissociated from frozen tissue, dispensing with the necessity to synchronize the tissue collection for all samples destined for the same scRNA-seq batch into a single day. In combination with a histone-associated eGFP mouse line, where the fluorophore is highly concentrated in the cell nuclei (59), snRNA-seq is therefore likely the best next step in the future iterations of this approach. Additionally, using the same fluorophore (i.e.,

eGFP) in both the control and KO cells would further standardize the cell sorting process. The improvements outlined above have the potential to further optimize this innovative approach to therapeutic target discovery by mapping transcriptional pathways associated with a complex neural disease, applicable to the study of genes beyond *Pten*.

Methods

Mouse *Pten* cKO and tissue collection

Dentate gyrus (DG) of *Pten*$^{flox/flox}$ mice was injected with retroviral particles carrying either GFP or mCherry-Cre constructs on post-natal day 7 as described by Williams *et al.* (25). The tissue was then collected 28 days post-injection, as described by Tasic et al. (60). Briefly, individual mice were anesthetized with 2% tribromoethanol (Avertin), perfused with artificial cerebrospinal fluid (ACSF), decapitated, and the brain was immediately removed and submerged in fresh ice-cold ACSF bubbled with carbogen gas (95% O_2 and 5% CO_2). The brain was sectioned on vibratome on ice, and each slice (300 µm) was immediately transferred to an ACSF bath at room temperature. DG was then microdissected under a microscope, and the slices after the dissection were visualized under a confocal microscope to verify the presence of the respective fluorophores. Subsequently, the cell dissociation protocol was carried out using the Papain Dissociation System (Worthington, LK003150), following the manufacturer's protocol. The dissociation protocol was optimized to yield at least 80% viable cells, as determined using Trypan Blue.

Flow cytometry and single-cell RNA sequencing

Single cells were isolated by fluorescence-activated cell sorting (FACS) on FACSAria III cell sorter using a 70 µm nozzle, sorting at 70 psi, in single-cell sorting mode, into phosphate-buffered saline (PBS) and stored on ice. To exclude dead cells, DAPI was added to the single-cell suspension to a final concentration of 2 ng/ml and FACS populations were chosen to select single cells with low DAPI (using the 405 nm laser) and high GFP (488 nm laser) or mCherry (561 nm laser) signal. The accuracy of sorting was confirmed by visually observing DAPI staining in the sorted cells. Sorted cells were then processed by the 10X Genomics Chromium workflow for scRNA-seq library construction and subsequently sequenced on Illumina NextSeq 500 sequencer.

Data analysis

The sequencing files were decomplexed and reads were aligned to the mm10 v3.0.0 Cell Ranger mouse reference genome using Cell Ranger v3.1 software. Subsequent data analysis was carried out in R using the Seurat package v4.0.5 (61). Only features detected in at least three cells were included as were only cells containing between $200 - 5,000$ genes total and no more than 20% mitochondrial genes. The data was subsequently normalized using regularized negative binomial regression (62). Cell types were detected with the python package ScNym (63), using an adversarial neural network model trained on TabulaMuris brain tissue data (64).

ACKNOWLEDGEMENTS

This research was supported by Bakala Foundation (M.S.), Rosaline Borison Memorial Fund (M.S.), Burroughs Wellcome Fund - Big Data in the Life Sciences Training Program at Dartmouth (M.S.), National Institutes of Health: DP1MH110234 (G.B.), Geisel School of Medicine at Dartmouth (G.B.). This article was written using the HenriquesLab bioRxiv template.

Bibliography

1. M. R. Nelen, G. W. Padberg, E. A.J. Peeters, A. Y. Lin, B. Van Den Helm, R. R. Frants, V. Coulon, A. M. Goldstein, M. M.M. Van Reen, D. F. Easton, R. A. Eeles, S. Hodgson, J. J. Mulvihill, V. A. Murday, M. A. Tucker, E. C.M. Mariman, T. M. Starink, B. A.J. Ponder, H. H. Ropers, H. Kremer, M. Longy, and C. Eng. Localization of the gene for Cowden disease to chromosome 10q22-23. *Nature Genetics*, 13(1):114–116, may 1996. ISSN 10614036. doi:10.1038/ng0596-114.
2. Dehe Kong, Akihiko Suzuki, Tong Tong Zou, Akira Sakurada, Lawrence W. Kemp, Shigeru Wakatsuki, Tadaaki Yokoyama, Hiromitsu Yamakawa, Toru Furukawa, Masami Sato, Noriaki Ohuchi, Shinji Sato, Jing Yin, Suna Wang, John M. Abraham, Rhonda F. Souza, Kara N. Smolinski, Stephen J. Meltzer, and Akira Horii. Pten1 is frequently mutated in primary endometrial carcinomas. *Nature Genetics*, 17(2):144, oct 1997. ISSN 15461718. doi:10.1038/ng1097-143.
3. Jorge A. Benitez, Jianhui Ma, Matteo D'Antonio, Antonia Boyer, Maria Fernanda Camargo, Ciro Zanca, Stephen Kelly, Alireza Khodadadi-Jamayran, Nathan M. Jameson, Michael Andersen, Hrvoje Miletic, Shahram Saberi, Kelly A. Frazer, Webster K. Cavenee, and Frank B. Furnari. PTEN regulates glioblastoma oncogenesis through chromatin-associated complexes of DAXX and histone H3.3. *Nature Communications*, 8:15223, may 2017. ISSN 20411723. doi:10.1038/ncomms15223.
4. Peter A. Steck, Mark A. Pershouse, Samar A. Jasser, W. K.Alfred Yung, Huai Lin, Azra H. Ligon, Lauren A. Langford, Michelle L. Baumgard, Thomas Hattier, Thaylon Davis, Cheryl Frye, Rong Hu, Bradley Swedlund, David H.F. Teng, and Scan V. Tavtigian. Identification of a candidate tumour suppressor gene, MMAC1, at chromosome 10q23.3 that is mutated in multiple advanced cancers. *Nature Genetics*, 15(4):356–362, apr 1997. ISSN 10614036. doi:10.1038/ng0497-356.
5. Natalie Jones, Françoise Bonnet, Sana Sfar, Marie Lafitte, Delfine Lafon, Ghislaine Sierankowski, Véronique Brouste, Guillaume Banneau, Christine Tunon De Lara, Marc Debled, Gaëtan MacGrogan, Michel Longy, and Nicolas Sevenet. Comprehensive analysis of PTEN status in breast carcinomas. *International Journal of Cancer*, 133(2):323–334, jul 2013. ISSN 00207136. doi:10.1002/ijc.28021.
6. J Li, C Yen, D Liaw, K Podsypanina, S Bose, S I Wang, J Puc, C Miliaresis, L Rodgers, R McCombie, S H Bigner, B C Giovanella, M Ittmann, B Tycko, H Hibshoosh, M H Wigler, and R Parsons. PTEN, a putative protein tyrosine phosphatase gene mutated in human brain, breast, and prostate cancer. *Science (New York, N.Y.)*, 275(5308):1943–7, mar 1997. ISSN 0036-8075. doi:10.1126/SCIENCE.275.5308.1943.
7. Jeffrey A. Engelman, Ji Luo, and Lewis C. Cantley. The evolution of phosphatidylinositol 3-kinases as regulators of growth and metabolism. *Nature Reviews Genetics*, 7(8):606–619, aug 2006. ISSN 14710056. doi:10.1038/nrg1879.
8. Debbie J. Marsh, Patricia L.M. Dahia, Zimu Zheng, Danny Liaw, Ramon Parsons, Robert J. Gorlin, and Charis Eng. Germline mutations in pten are present in bannayan-zonana syndrome. *Nature Genetics*, 16(4):333–334, 1997. ISSN 15461718. doi:10.1038/ng0897-333.
9. Xiao Ping Zhou, Heather Hampel, Hannelore Thiele, Robert J. Gorlin, Raoul C.M. Hennekam, Melissa Parisi, Robin M. Winter, and Charis Eng. Association of germline mutation in the PTEN tumour suppressor gene and Proteus and Proteus-like syndromes. *Lancet*, 358(9277):210–211, 2001. ISSN 01406736. doi:10.1016/S0140-6736(01)05412-5.
10. X. P. Zhou, D. J. Marsh, H. Hampel, J. B. Mulliken, O. Gimm, and C. Eng. Germline and germline mosaic PTEN mutations associated with a Proteus-like syndrome of hemihypertrophy, lower limb asymmetry, arteriovenous malformations and lipomatosis. *Human Molecular Genetics*, 9(5):765–8, 2000.
11. Debbie J. Marsh, Jennifer B. Kum, Kathryn L. Lunetta, Michael J. Bennett, Robert J. Gorlin, S. Faisal Ahmed, Joann Bodurtha, Carol Crowe, Mary A. Curtis, Majed Dasouki, Teresa Dunn, Howard Feit, Michael T. Geraghty, John M. Graham, Shirley V. Hodgson, Alasdair Hunter, Bruce R. Korf, David Manchester, Susan Miesfeldt, Victoria A. Murday, Katherine L. Nathanson, Melissa Parisi, Barbara Pober, Corrado Romano, John L. Tolmie, Richard Trembath, Robin M. Winter, Elaine H. Zackai, Roberto T. Zori, Liang Ping Weng, Patricia L.M. Dahia, and Charis Eng. PTEN mutation spectrum and genotype-phenotype correlations in Bannayan-Riley-Ruvalcaba syndrome suggest a sin-

gle entity with Cowden syndrome. *Human Molecular Genetics*, 8(8):1461–1472, 1999. ISSN 09646906. doi:10.1093/hmg/8.8.1461.

12. Charis Eng. PTEN: One gene, Many syndromes. *Human Mutation*, 22(3): 183–198, sep 2003. ISSN 10597794. doi:10.1002/humu.10257.
13. Roberto T. Zori, Debbie J. Marsh, Gail E. Graham, Errol B. Marliss, and Charis Eng. Germline PTEN mutation in a family with Cowden syndrome and Bannayan-Riley-Ruvalcaba Syndrome. *American Journal of Medical Genetics*, 80(4):399–402, dec 1998. ISSN 0148-7299. doi:10.1002/(SICI)1096-8628(19981204)80:4<399::AID-AJMG18>3.0.CO;2-O.
14. Claudia Perandones, Roxana Verónica Costanzo, Valeria Kowaljow, Omar Hilario Pivetta, Hector Carminatti, and Martín Radrizzani. Correlation between synaptogenesis and the PTEN phosphatase expression in dendrites during postnatal brain development. *Molecular Brain Research*, 128(1):8–19, sep 2004. ISSN 0169328X. doi:10.1016/j.molbrainres.2004.05.021.
15. Elizabeth A. Varga, Matthew Pastore, Thomas Prior, Gail E. Herman, and Kim L. McBride. The prevalence of PTEN mutations in a clinical pediatric cohort with autism spectrum disorders, developmental delay, and macrocephaly. *Genetics in Medicine*, 11(2):111–117, feb 2009. ISSN 10983600. doi:10.1097/GIM.0b013e31818fd762.
16. T. W. Frazier, R. Embacher, A. K. Tilot, K. Koenig, J. Mester, and C. Eng. Molecular and phenotypic abnormalities in individuals with germline heterozygous PTEN mutations and autism. *Molecular Psychiatry*, 20(9):1132–1138, 2015. ISSN 14765578. doi:10.1038/mp.2014.125.
17. M. P. Myers, J. P. Stolarov, C. Eng, J. Li, S. I. Wang, M. H. Wigler, R. Parsons, and N. K. Tonks. P-TEN, the tumor suppressor from human chromosome 10q23, is a dual-specificity phosphatase. *Proceedings of the National Academy of Sciences*, 94(17):9052–9057, aug 1997. ISSN 0027-8424. doi:10.1073/pnas.94.17.9052.
18. D. C I Goberdhan, Nuria Paricio, Emma C. Goodman, Marek Mlodzik, and Clive Wilson. Drosophila tumor suppressor PTEN controls cell size and number by antagonizing the Chico/PI3-kinase signaling pathway. *Genes and Development*, 13(24):3244–3258, dec 1999. ISSN 08909369. doi:10.1101/gad.13.24.3244.
19. Sandra Jurado, Marion Benoist, Argentina Lario, Shira Knafo, Cortney N. Petrok, and José A. Esteban. PTEN is recruited to the postsynaptic terminal for NMDA receptor-dependent long-term depression. *EMBO Journal*, 29 (16):2827–2840, aug 2010. ISSN 02614189. doi:10.1038/emboj.2010.160.
20. Catherine J. Fricano-Kugler, Stephanie A. Getz, Michael R. Williams, Ashley A. Zurawel, Tyrone DeSpenza, Paul W. Frazel, Meijie Li, Alistair J. O'Malley, Erika L. Moen, and Bryan W. Luikart. Nuclear Excluded Autism-Associated Phosphatase and Tensin Homolog Mutations Dysregulate Neuronal Growth. *Biological Psychiatry*, 2018. ISSN 18732402. doi:10.1016/j.biopsych.2017.11.025.
21. Chang-Hyuk Kwon, Xiaoyan Zhu, Junyuan Zhang, Lori L. Knoop, Ruby Tharp, Richard J. Smeyne, Charles G. Eberhart, Peter C. Burger, and Suzanne J. Baker. Pten regulates neuronal soma size: a mouse model of Lhermitte-Duclos disease. *Nature Genetics*, 29(4):404–411, dec 2001. ISSN 1061-4036. doi:10.1038/ng781.
22. Matthias Groszer, Rebecca Erickson, Deirdre D Scripture-adams, Ralf Lesche, Andreas Trumpp, Jerome A Zack, Harley I Kornblum, Xin Liu, and Hong Wu. Negative Regulation of Neural Stem/Progenitor Cell Proliferation by the Pten Tumor Suppressor Gene in Vivo. *Science*, 294(December):2186–2189, 2001.
23. Chang Hyuk Kwon, Bryan W. Luikart, Craig M. Powell, Jing Zhou, Sharon A. Matheny, Wei Zhang, Yanjiao Li, Suzanne J. Baker, and Luis F. Parada. Pten Regulates Neuronal Arborization and Social Interaction in Mice. *Neuron*, 50 (3):377–388, may 2006. ISSN 08966273. doi:10.1016/j.neuron.2006.03.023.
24. B. W. Luikart, E. Schnell, E. K. Washburn, A. L. Bensen, K. R. Tovar, and G. L. Westbrook. Pten Knockdown In Vivo Increases Excitatory Drive onto Dentate Granule Cells. *Journal of Neuroscience*, 31(11):4345–4354, mar 2011. ISSN 0270-6474. doi:10.1523/JNEUROSCI.0061-11.2011.
25. M. R. Williams, T. DeSpenza, M. Li, A. T. Gulledge, and B. W. Luikart. Hyperactivity of Newborn Pten Knock-out Neurons Results from Increased Excitatory Synaptic Drive. *Journal of Neuroscience*, 35(3):943–959, jan 2015. ISSN 0270-6474. doi:10.1523/JNEUROSCI.3144-14.2015.
26. Jingwen Lyu, Xiuya Yu, Lingjie He, Tianlin Cheng, Jingjing Zhou, Cheng Cheng, Zhifang Chen, Guoqiang Cheng, Zilong Qiu, and Wenhao Zhou. The protein phosphatase activity of PTEN is essential for regulating neural stem cell differentiation. *Molecular Brain*, 8(1):26, apr 2015. ISSN 17566606. doi:10.1186/s13041-015-0114-1.
27. Antonio Di Cristofano, Barbara Pesce, Carlos Cordon-Cardo, and Pier Paolo Pandolfi. Pten is essential for embryonic development and tumour suppression. *Nature Genetics*, 19(4):348–355, aug 1998. ISSN 10614036. doi:10.1038/1235.
28. Akira Suzuki, José Luis de la Pompa, Vuk Stambolic, Andrew J. Elia, Takehiko Sasaki, Ivén del Barco Barrantes, Alexandra Ho, Andrew Wakeham, Annick Ltie, Wilson Khoo, Manabu Fukumoto, and Tak W. Mak. High cancer susceptibility and embryonic lethality associated with mutation of the PTEN tumor suppressor gene in mice. *Current Biology*, 8(21):1169–1178, oct 1998. ISSN 0960-9822. doi:10.1016/S0960-9822(07)00488-5.
29. K Podsypanina, L H Ellenson, A Nemes, J Gu, M Tamura, K M Yamada, C Cordon-Cardo, G Catoretti, P E Fisher, and R Parsons. Mutation of Pten/Mmac1 in mice causes neoplasia in multiple organ systems. *Proceedings of the National Academy of Sciences of the United States of America*, 96 (4):1563–8, feb 1999. ISSN 0027-8424. doi:10.1073/PNAS.96.4.1563.
30. Akira Suzuki, Manae Tsukio Yamaguchi, Toshiaki Ohteki, Takehiko Sasaki, Tsuneyasu Kaisho, Yuki Kimura, Ritsuko Yoshida, Andrew Wakeham, Tetsuya Higuchi, Manabu Fukumoto, Takeshi Tsubata, Pamela S Ohashi, Shigeo Koyasu, Josef M Penninger, Toru Nakano, and Tak W Mak. T Cell-Specific Loss of Pten Leads to Defects in Central and Peripheral Tolerance. *Immunity*, 14(5): 523–534, may 2001. ISSN 1074-7613. doi:10.1016/S1074-7613(01)00134-0.
31. Jessica L. Mester, Amanda K. Tilot, Lisa A. Rybicki, Thomas W. Frazier, and Charis Eng. Analysis of prevalence and degree of macrocephaly in patients with germline PTEN mutations and of brain weight in Pten knock-in murine model. *European Journal of Human Genetics*, 19(7):763–768, jul 2011. ISSN 10184813. doi:10.1038/ejhg.2011.20.
32. Amy E. Clipperton-Allen and Damon T. Page. Pten haploinsufficient mice show broad brain overgrowth but selective impairments in autism-relevant behavioral tests. *Human Molecular Genetics*, 23(13):3490–3505, jul 2014. ISSN 14602083. doi:10.1093/hmg/ddu057.
33. Tomohiko Maehama and Jack E. Dixon. The tumor suppressor, PTEN/MMAC1, dephosphorylates the lipid second messenger, phosphatidylinositol 3,4,5-trisphosphate. *Journal of Biological Chemistry*, 273(22):13375–13378, may 1998. ISSN 00219258. doi:10.1074/jbc.273.22.13375.
34. Vuk Stambolic, Akira Suzuki, José Luis de la Pompa, Greg M Brothers, Christine Mirtsos, Takehiko Sasaki, Jurgen Ruland, Josef M Penninger, David P Siderovski, and Tak W Mak. Negative Regulation of PKB/Akt-Dependent Cell Survival by the Tumor Suppressor PTEN. *Cell*, 95(1):29–39, oct 1998. ISSN 0092-8674. doi:10.1016/S0092-8674(00)81780-8.
35. Xinyi Wu, Kristen Senechal, Mehran S. Neshat, Young E. Whang, and Charles L. Sawyers. The PTEN/MMAC1 tumor suppressor phosphatase functions as a negative regulator of the phosphoinositide 3-kinase/Akt pathway. *Proceedings of the National Academy of Sciences*, 95(26):15587–15591, dec 1998. ISSN 0027-8424. doi:10.1073/PNAS.95.26.15587.
36. Stephanie A. Getz, Tyrone DeSpenza, Meijie Li, and Bryan W. Luikart. Rapamycin prevents, but does not reverse, aberrant migration in Pten knockout neurons. *Neurobiology of Disease*, 93:12–20, sep 2016. ISSN 1095953X. doi:10.1016/j.nbd.2016.03.010.
37. M Tamura, J Gu, K Matsumoto, S Aota, R Parsons, and K M Yamada. Inhibition of cell migration, spreading, and focal adhesions by tumor suppressor PTEN. *Science (New York, N.Y.)*, 280(5369):1614–7, jun 1998. ISSN 0036-8075. doi:10.1126/SCIENCE.280.5369.1614.
38. J Gu, M Tamura, R Pankov, E H Danen, T Takino, K Matsumoto, and K M Yamada. Shc and FAK differentially regulate cell motility and directionality modulated by PTEN. *The Journal of cell biology*, 146(2):389–403, jul 1999. ISSN 0021-9525. doi:10.1083/JCB.146.2.389.
39. Tingting Gu, Zhong Zhang, Jianli Wang, Junyi Guo, Wen Hong Shen, and Yuxin Yin. CREB is a novel nuclear target of PTEN phosphatase. *Cancer research*, 71(8):2821–5, apr 2011. ISSN 1538-7445. doi:10.1158/0008-5472.CAN-10-3399.
40. Xiaoqun Catherine Zhang, Antonella Piccini, Michael P. Myers, Linda Van Aelst, and Nicholas K. Tonks. Functional analysis of the protein phosphatase activity of PTEN. *Biochemical Journal*, 444(3):457–464, jun 2012. ISSN 0264-6021. doi:10.1042/BJ20120098.
41. Priyanka Tibarewal, Georgios Zilidis, Laura Spinelli, Nick Schurch, Helene Maccario, Alexander Gray, Nevin M Perera, Lindsay Davidson, Geoffrey J Barton, and Nick R Leslie. PTEN protein phosphatase activity correlates with control of gene expression and invasion, a tumor-suppressing phenotype, but not with AKT activity. *Science signaling*, 5(213):ra18, feb 2012. ISSN 1937-9145. doi:10.1126/scisignal.2002138.
42. Yuji Shi, Junru Wang, Sarat Chandarlapaty, Justin Cross, Craig Thompson, Neal Rosen, and Xuejun Jiang. PTEN is a protein tyrosine phosphatase for IRS1. *Nature Structural & Molecular Biology*, 21(6):522–527, jun 2014. ISSN 1545-9993. doi:10.1038/nsmb.2828.
43. Xiaojie Qiu, Qi Mao, Ying Tang, Li Wang, Raghav Chawla, Hannah A. Pliner, and Cole Trapnell. Reversed graph embedding resolves complex single-cell trajectories. *Nature Methods*, 14(10):979–982, 2017. ISSN 15487105. doi:10.1038/nmeth.4402.
44. Sébastien Jacquemont, Bradley P. Coe, Micha Hersch, Michael H. Duyzend, Niklas Krumm, Sven Bergmann, Jacques S. Beckmann, Jill A. Rosenfeld, and Evan E. Eichler. A higher mutational burden in females supports a "female protective model" in neurodevelopmental disorders. *American Journal of Human Genetics*, 94(3):415–425, mar 2014. ISSN 15376605.

doi:10.1016/j.ajhg.2014.02.001.

45. Jon Baio, Lisa Wiggins, Deborah L. Christensen, Matthew J Maenner, Julie Daniels, Zachary Warren, Margaret Kurzius-Spencer, Walter Zahorodny, Cordelia Robinson, Rosenberg, Tiffany White, Maureen S. Durkin, Pamela Imm, Loizos Nikolaou, Marshalyn Yeargin-Allsopp, Li-Ching Lee, Rebecca Harrington, Maya Lopez, Robert T. Fitzgerald, Amy Hewitt, Sydney Pettygrove, John N. Constantino, Alison Vehorn, Josephine Shenouda, Jennifer Hall-Lande, Kim Van, Naarden, Braun, and Nicole F. Dowling. Prevalence of Autism Spectrum Disorder Among Children Aged 8 Years — Autism and Developmental Disabilities Monitoring Network, 11 Sites, United States, 2014. *MMWR. Surveillance Summaries*, 67(6):1–23, 2018. ISSN 1546-0738. doi:10.15585/mmwr.ss6706a1.
46. Aleide Goffin, Lies H. Hoefsloot, Ermanno Bosgoed, Ann Swillen, and Jean Pierre Fryns. PTEN mutation in a family with Cowden syndrome and autism. *American Journal of Medical Genetics - Neuropsychiatric Genetics*, 105(6):521–524, aug 2001. ISSN 15524841. doi:10.1002/ajmg.1477.
47. Emily Hansen-Kiss, Sarah Beinkampen, Brent Adler, Thomas Frazier, Thomas Prior, Steven Erdman, Charis Eng, and Gail Herman. A retrospective chart review of the features of PTEN hamartoma tumour syndrome in children. *Journal of Medical Genetics*, 54(7):471–478, 2017. ISSN 14686244. doi:10.1136/jmedgenet-2016-104484.
48. Amanda K. Tilot, Mary K. Gaugler, Qi Yu, Todd Romigh, Wanfeng Yu, Robert H. Miller, Thomas W. Frazier, and Charis Eng. Germline disruption of Pten localization causes enhanced sex-dependent social motivation and increased glial production. *Human Molecular Genetics*, 23(12):3212–3227, jun 2014. ISSN 14602083. doi:10.1093/hmg/ddu031.
49. Dan Freeman, Ralf Lesche, Nathalie Kertesz, Shungyou Wang, Gang Li, Jing Gao, Matthias Groszer, Hilda Martinez-Diaz, Nora Rozengurt, George Thomas, Xin Liu, and Hong Wu. Genetic background controls tumor development in Pten-deficient mice. *Cancer Research*, 66(13):6492–6496, mar 2006. ISSN 00085472. doi:10.1158/0008-5472.CAN-05-4143.
50. Ji Hyun Chung, Margaret E. Ginn-Pease, and Charis Eng. Phosphatase and tensin homologue deleted on chromosome 10 (PTEN) has nuclear localization signal-like sequences for nuclear import mediated by major vault protein. *Cancer Research*, 65(10):4108–4116, may 2005. ISSN 00085472. doi:10.1158/0008-5472.CAN-05-0124.
51. Salah Ayoub, Benedikt Obermayer, F. Alexander Wolf, Christine Kocks, Aristotelis Misios, Jordi Solana, Petar Glažar, Nikolaus Rajewsky, Mireya Plass, and Fabian J. Theis. Cell type atlas and lineage tree of a whole complex animal by single-cell transcriptomics. *Science*, 360(6391):eaaq1723, 2018. ISSN 0036-8075. doi:10.1126/science.aaq1723.
52. Hidenori Ito, Rika Morishita, and Koh-ichi Nagata. Autism spectrum disorder-associated genes and the development of dentate granule cells. *Medical Molecular Morphology*, 50(3):123–129, sep 2017. ISSN 1860-1480. doi:10.1007/s00795-017-0161-z.
53. Fiorenza Stagni, Andrea Giacomini, Sandra Guidi, Elisabetta Ciani, and Renata Bartesaghi. Timing of therapies for Down syndrome: the sooner, the better. *Frontiers in Behavioral Neuroscience*, 9:265, oct 2015. ISSN 1662-5153. doi:10.3389/fnbeh.2015.00265.
54. Tomislav Ilicic, Jong Kyoung Kim, Aleksandra A. Kolodziejczyk, Frederik Otzen Bagger, Davis James McCarthy, John C. Marioni, and Sarah A. Teichmann. Classification of low quality cells from single-cell RNA-seq data. *Genome Biology*, 17(1):1–15, 2016. ISSN 1474760X. doi:10.1186/s13059-016-0888-1.
55. Serena Grossi, Stefano Regis, Roberta Biancheri, Matthew Mort, Susanna Lualdi, Enrico Bertini, Graziella Uziel, Odile Boespflug-Tanguy, Alessandro Simonati, Fabio Corsolini, Ercan Demir, Valentina Marchiani, Antonio Percesepe, Franco Stanzial, Andrea Rossi, Catherine Vaurs-Barrière, David N. Cooper, and Mirella Filocamo. Molecular Genetic Analysis of the PLP1 Gene in 38 Families with PLP1-related disorders: Identification and Functional Characterization of 11 Novel PLP1 Mutations. *Orphanet Journal of Rare Diseases*, 6(1): 1–13, jun 2011. ISSN 17501172. doi:10.1186/1750-1172-6-40/FIGURES/2.
56. Cefan Zhou, Ming Wang, Jing Yang, Hui Xiong, Yefu Wang, and Jingfeng Tang. Integral membrane protein 2A inhibits cell growth in human breast cancer via enhancing autophagy induction. *Cell Communication and Signaling*, 17(1):1–14, aug 2019. ISSN 1478811X. doi:10.1186/S12964-019-0422-7/FIGURES/4.
57. J M Zarling, M Shoyab, H Marquardt, M B Hanson, M N Lioubin, and G J Todaro. Oncostatin M: a growth regulator produced by differentiated histiocytic lymphoma cells. *Proceedings of the National Academy of Sciences of the United States of America*, 83(24):9739–43, dec 1986. ISSN 0027-8424. doi:10.1073/pnas.83.24.9739.
58. Trygve E. Bakken, Rebecca D. Hodge, Jeremy A. Miller, Zizhen Yao, Thuc Nghi Nguyen, Brian Aevermann, Eliza Barkan, Darren Bertagnolli, Tamara Casper, Nick Dee, Emma Garren, Jeff Goldy, Lucas T. Graybuck, Matthew Kroll, Roger S. Lasken, Kanan Lathia, Sheana Parry, Christine Rimorin, Richard H. Scheuermann, Nicholas J. Schork, Soraya I. Shehata, Michael Tieu, John W. Phillips, Amy Bernard, Kimberly A. Smith, Hongkui Zeng, Ed S. Lein, and Bosiljka Tasic. Single-nucleus and single-cell transcriptomes compared in matched cortical cell types. *PLOS ONE*, 13(12):e0209648, dec 2018. ISSN 1932-6203. doi:10.1371/journal.pone.0209648.
59. Partha Samadder, Ning Weng, Thomas Doetschman, Ronald L. Heimark, and David W. Galbraith. Flow cytometry and single nucleus sorting for Cre-based analysis of changes in transcriptional states. *Cytometry Part A*, 89(5):430–442, 2016. ISSN 15524930. doi:10.1002/cyto.a.22847.
60. Bosiljka Tasic, Vilas Menon, Thuc Nghi Nguyen, Tae Kyung Kim, Tim Jarsky, Zizhen Yao, Boaz Levi, Lucas T Gray, Staci A Sorensen, Tim Dolbeare, Darren Bertagnolli, Jeff Goldy, Nadiya Shapovalova, Sheana Parry, Changkyu Lee, Kimberly Smith, Amy Bernard, Linda Madisen, Susan M Sunkin, Michael Hawrylycz, Christof Koch, and Hongkui Zeng. Adult mouse cortical cell taxonomy revealed by single cell transcriptomics. *Nature Neuroscience*, 19(2): 335–346, feb 2016. ISSN 1097-6256. doi:10.1038/nn.4216.
61. Yuhan Hao, Stephanie Hao, Erica Andersen-Nissen, William M. Mauck, Shiwei Zheng, Andrew Butler, Maddie J. Lee, Aaron J. Wilk, Charlotte Darby, Michael Zager, Paul Hoffman, Marlon Stoeckius, Efthymia Papalexi, Eleni P. Mimitou, Jaison Jain, Avi Srivastava, Tim Stuart, Lamar M. Fleming, Bertrand Yeung, Angela J. Rogers, Juliana M. McElrath, Catherine A. Blish, Raphael Gottardo, Peter Smibert, and Rahul Satija. Integrated analysis of multimodal single-cell data. *Cell*, 184(13):3573–3587.e29, jun 2021. ISSN 0092-8674. doi:10.1016/J.CELL.2021.04.048.
62. Christoph Hafemeister and Rahul Satija. Normalization and variance stabilization of single-cell RNA-seq data using regularized negative binomial regression. *Genome Biology*, 20(1):296, dec 2019. ISSN 1474-760X. doi:10.1186/s13059-019-1874-1.
63. Jacob C. Kimmel and David R. Kelley. Semisupervised adversarial neural networks for single-cell classification. *Genome Research*, 31(10):1781–1793, oct 2021. ISSN 1088-9051. doi:10.1101/GR.268581.120.
64. The Tabula Muris Consortium. Single-cell transcriptomics of 20 mouse organs creates a Tabula Muris. *Nature*, 562(7727):367–372, oct 2018. ISSN 0028-0836. doi:10.1038/s41586-018-0590-4.